











## Transient guided-mode resonance metasurfaces with phase-transition materials

DOMENICO DE CEGLIA,<sup>1,2,\*</sup>  MARCO GANDOLFI,<sup>1,2</sup>  MARIA ANTONIETTA VINCENTI,<sup>1,2</sup>   
ANDREA TOGNAZZI,<sup>2,3</sup>  PAOLO FRANCESCHINI,<sup>1,2</sup>  ALFONSO C. CINO,<sup>3</sup> GINA AMBROSIO,<sup>2</sup>  
CAMILLA BARATTO,<sup>2</sup> BOHAN LI,<sup>4</sup> ROCIO CAMACHO-MORALES,<sup>4</sup>  DRAGMOIR N. NESHEV,<sup>4</sup>   
AND COSTANTINO DE ANGELIS<sup>1,2</sup> 

<sup>1</sup>Department of Information Engineering, University of Brescia, Via Branze 38, Brescia, 25123, Italy

<sup>2</sup>Istituto Nazionale di Ottica - Consiglio Nazionale delle Ricerche, Via Branze 45, Brescia, 25123, Italy

<sup>3</sup>Department of Engineering, University of Palermo, Viale delle Scienze ed. 9, Palermo, 90128, Italy

<sup>4</sup>ARC Centre of Excellence for Transformative Meta-Optical Systems (TMOS), Department of Electronic Materials Engineering, Research School of Physics, The Australian National University, Canberra, ACT 2601, Australia

\*domenico.deceglia@unibs.it

Received 31 January 2023; revised 6 April 2023; accepted 11 May 2023; posted 11 May 2023; published 25 May 2023

We investigate transient, photo-thermally induced metasurface effects in a planar thin-film multilayer based on a phase-transition material. Illumination of a properly designed multilayer with two obliquely incident and phase-coherent pulsed pumps induces a transient and reversible temperature pattern in the phase-transition layer. The deep periodic modulation of the refractive index, caused by the interfering pumps, produces a transient Fano-like spectral feature associated with a guided-mode resonance. A coupled opto-thermal model is employed to analyze the temporal dynamics of the transient metasurface and to evaluate its speed and modulation capabilities. Using near-infrared pump pulses with peak intensities of the order of 100 MW/cm<sup>2</sup> and duration of a few picoseconds, we find that the characteristic time scale of the transient metasurface is of the order of nanoseconds. Our results indicate that inducing transient metasurface effects in films of phase-transition materials can lead to new opportunities for dynamic control of quality ( $Q$ )-factor in photonic resonances, and for light modulation and switching. © 2023 Optica Publishing Group

<https://doi.org/10.1364/OL.486733>

**Introduction.** Metasurfaces are ultrathin planar structures that can be used for wavefront engineering. The angular and frequency responses of a metasurface are encoded in its planar pattern, and, therefore, the metasurface functionalities are typically set at the time of fabrication. Gratings supporting high-quality ( $Q$ ) resonances are periodic structures that can be regarded as nonlocal metasurfaces [1]. Indeed, the periodicity of a grating introduces an additional transverse momentum to impinging light, and it enables coupling to modes with long lifetime and large extension over the plane of the grating. Nonlocal metasurfaces can be either diffractive (metagratings), when the periodicity is superwavelength, or nondiffractive (zeroth-order gratings), when the periodicity is subwavelength. Periodic perturbations of refractive index in gratings are typically achieved

by fabricating arrangements of slits or grooves in the plane of the structure. If a continuous, single or multilayer film supports a guided mode in the plane of the film, then the introduction of a periodic perturbation of the refractive index may generate an abrupt change of reflectance and transmittance of plane waves near a specific wavelength, known as Wood-Rayleigh anomaly [2]. The anomaly is due to the resonant coupling of an evanescent diffracted order to the guided mode [3]. This kind of anomaly is known as guided-mode resonance (GMR). GMRs manifest themselves as asymmetric, Fano-like features [4] in the frequency and angular spectra of plane waves illuminating the grating. In a one-dimensional grating, coupling to a GMR mode is ruled by the phase-matching requirement:  $\beta = k_{\parallel} + m2\pi/p$ , where  $\beta$  is the guided mode propagation constant,  $k_{\parallel}$  is the incident plane wave wave vector component parallel to the plane of the grating,  $p$  is the grating periodicity, and  $m$  is the diffraction order [5–8]. Without the periodic perturbation, the mode is “dark” for plane wave excitation, since the propagation constant  $\beta$  exceeds  $k_{\parallel}$ . GMRs act as highly selective wavelength and angular filters. Devices based on GMRs include optical sensors, filters, mirrors, switches, modulators, as well as nanoscale frequency mixers exploiting the large electric-field enhancement and light confinement at the resonance [9,10].

The response of nonlocal GMR metasurfaces is ruled by their periodicity. Endowing these structures with the ability to dynamically change the periodicity is highly desirable to develop reconfigurable and tunable functionalities for applications that range from radio frequency and visible-light communications to microscopy and analog optical computing. Instead of introducing gratings by permanently modifying the geometry of the planar structures, one can induce them in a volatile way by exciting a properly designed system with an external control light (pump). For example, by applying interfering pumps to a planar structure and exploiting photo-acoustic or photo-thermal effects, a transient grating can be generated that disappears when the pump light is switched off. Transient diffraction gratings are

employed for spectroscopy in materials science and chemistry [11]. In transient grating spectroscopy, an interference pattern induced by two obliquely incident and phase-coherent pumps generates a spatial refractive-index modulation on a film, which then diffracts the light of a probe signal into the first diffraction order. This tool is used to examine the electronic and phononic responses of complex materials, as well as for molecular dynamics [12–14]. The onset of the first diffraction order in a transient grating induced on a single film of vanadium dioxide ( $\text{VO}_2$ ) has been observed in the ultraviolet [15]. Here we leverage the use of interfering pumps to induce GMR metasurface effects in unpatterned planar multilayers, and to dynamically control the  $Q$ -factor and the free-space coupling to nanophotonic resonances. Since a large index modulation is required to efficiently couple light to a GMR, we consider a planar multilayer based on a phase-transition material (PTM), which, under proper external stimuli, undergoes an abrupt phase change that strongly modifies its optical properties. Indeed, PTMs are recently receiving increasing attention for their ability to tune the electromagnetic response of photonic nanostructures [16–21]. In the proposed structure, the key elements to induce the transient metasurface effect are the following: (i) the presence of a “dark” guided mode supported by the multilayer; (ii) an illumination scheme with two interfering pumps; (iii) deep index modulation “written” in the PTM film when the interfering pumps are active. We confirm these mechanisms by using an opto-thermal model. We estimate that the characteristic lifetime of the GMR metasurface effect generated by pump pulses with duration of a few picoseconds is of the order of a few nanoseconds for a multilayer composed by a slab of silicon covered by a thin film of  $\text{VO}_2$ .

**Device concept and structure.** A sketch of the proposed induced transient metasurface device is illustrated in Fig. 1. A high-index planar layer acting as a waveguide is covered with a thin film of  $\text{VO}_2$  and sits on a lower-index substrate. The waveguide film is made of crystalline silicon (Si), which is known to be compatible with the growth of high-quality  $\text{VO}_2$  films [22], while the substrate is made of  $\text{SiO}_2$ .  $\text{VO}_2$  is a PTM with a dielectric (monoclinic) to metallic (tetragonal) phase transition, occurring, in the bulk form, at a critical temperature  $T_c = 67^\circ\text{C}$  [23]. When this temperature is reached, an abrupt variation of the material electrical conductivity can be observed, with a significant modulation of refractive index at optical wavelengths [24]. In the infrared, including telecommunications wavelengths, the

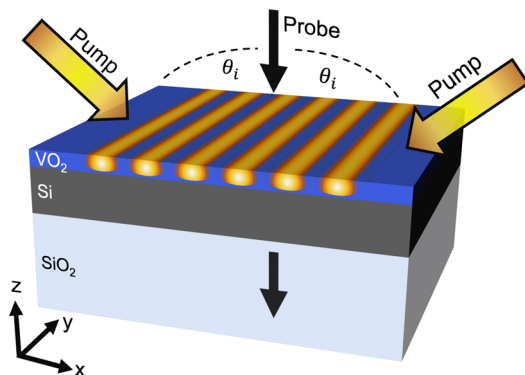


**Fig. 1.** Schematics of the multilayer and excitation mechanism: two pulsed and phase-coherent pump beams excite the structure at oblique incidence ( $\theta_i$ ). The probe at normal incidence experiences the transient GMR metasurface effect induced by the spatial interference pattern generated by the pump pulses.

material is insulating/transparent below  $T_c$ , and opaque/metallic above  $T_c$ . The transition can be induced with different kinds of stimuli, including optical radiation [25], and it is volatile. For example, upon the application of direct or indirect heating, the material will switch from insulating to metallic, while it will return to its initial state after the stimulus stops. In the proposed device, the structure is illuminated with a combination of two interfering pumps, tuned in the absorption range of  $\text{VO}_2$ , and a probe, as illustrated in Fig. 1. At equilibrium, i.e., without the application of the pumps, the system is an unpatterned planar thin film and, therefore, supports only broadband Fabry–Pérot resonances for a probe signal that is normally incident upon the multilayer. When the two obliquely incident coherent pumps are applied, an interference pattern of bright and dark regions will form on the structure. Due to absorption in the  $\text{VO}_2$  film, the interfering pumps produce a periodic temperature profile, as indicated in Fig. 1. When the intensity of the pumps is sufficiently large to locally trigger the phase transition in the PTM layer, the fingerprint of the temperature spatial profile is a periodic perturbation of the  $\text{VO}_2$  refractive index. In this way, a transient metasurface grating can be photo-thermally induced. Transient metasurface effects are probed with a plane wave at normal incidence, i.e., the probe signal. The shape and size of the grating can be modulated by varying the peak intensity of the pumps, their time duration, the angle of incidence, and the wavelength of the pumps. In the illustrative example discussed here, the pumps are both  $y$ -polarized and produce an overall incident electric field with a complex vector  $\vec{E}_p = \hat{y}2E_0 \cos(k_x x) e^{ik_z z}$ , where  $k_x = 2\pi/\lambda_0 \sin(\theta_i)$  and  $k_z = 2\pi/\lambda_0 \cos(\theta_i)$  are the wave vector components in the  $x$  and  $z$  directions, respectively,  $\lambda_0$  is the free-space wavelength of the pump,  $\theta_i$  the angle of incidence, and  $E_0$  the electric field amplitude of each pump. Since the absorption is proportional to the square of the pump field amplitude, the periodicity of the induced grating in the  $x$  direction is  $p = \lambda_0/[2 \sin(\theta_i)]$ . We have designed the structure to obtain the GMR metasurface effect in the near infrared while keeping an appropriate light confinement of the pump field in the  $\text{VO}_2$  film (see Supplement 1 for details). In particular, for a pump wavelength at  $\lambda_0 = 940$  nm and angle of incidence  $\theta_i = 44^\circ$ , the periodicity of the induced grating is  $p \approx 675$  nm. According to the phase-matching condition, the GMR is expected at a wavelength  $\lambda_{\text{GMR}} = p \times n_G$ , where  $n_G = \beta\lambda_0/(2\pi)$  is the effective index of the  $\text{TE}_0$  mode of the air- $\text{VO}_2$ -Si- $\text{SiO}_2$  slab waveguide. For an Si and  $\text{VO}_2$  film thickness of 200 nm and 75 nm, respectively, the guided mode effective index (calculated as outlined in [26]) is  $n_G \approx 2.86$  and, therefore,  $\lambda_{\text{GMR}} = 1.93$   $\mu\text{m}$ . The GMR wavelength can be controlled by changing the pump wavelength  $\lambda_0$  and the angle of incidence  $\theta_i$ . In other words, the transient non-diffractive, nonlocal metasurface effect mediated by the GMR is expected for probe wavelengths near  $\lambda_{\text{GMR}}$ .

**Results.** To obtain the transient response of the structure, we use a fully coupled opto-thermal model [20,27]. In our model, before light excitation, the device is at equilibrium at room temperature ( $T_{\text{amb}} = 20^\circ\text{C}$ ). Then, the pump pulses induce a light dissipation and heat generation, yielding a transient temperature increase in the system and a temporary modification of the  $\text{VO}_2$  refractive index. This index modulation is used to compute the new optical response of the structure both at pump and probe wavelengths, in a self-consistent way. In the simulations, we consider pump pulses with Gaussian temporal shape, with time duration (full width at half maximum of the intensity profile)  $\tau = 10$  ps and peak intensity  $I_0$  occurring at the time  $t_0 = 10\tau$ .

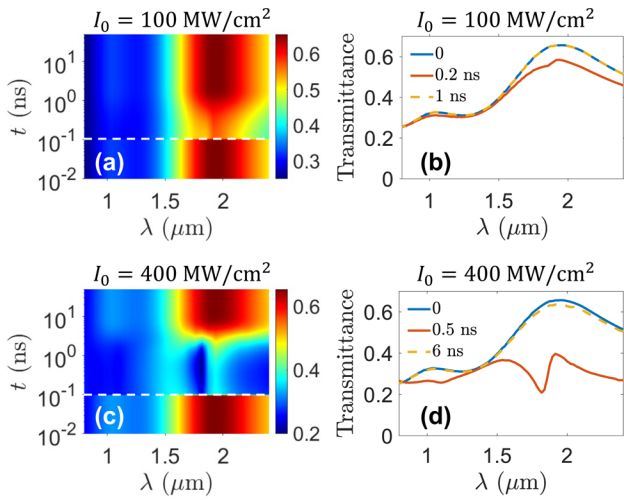


**Fig. 2.** Time evolution of the probe transmittance for two values of the pump peak intensity. (a),(b)  $I_0 = 100 \text{ MW/cm}^2$  and (c),(d)  $I_0 = 400 \text{ MW/cm}^2$ . Panels (b) and (d) report the probe spectra for the same values of pump peak intensities as in panels (a) and (c), and at three different instants: at equilibrium (blue curves,  $t = 0$ ), during the transition [red curves,  $t = 0.2 \text{ ns}$  in panel (b) and  $t = 0.5 \text{ ns}$  in panel (d)], and when  $\text{VO}_2$  switches back to its initial state [yellow dashed curves,  $t = 1 \text{ ns}$  in panel (b) and  $t = 6 \text{ ns}$  in panel (d)]. Dashed horizontal lines in panels (a) and (c) indicate  $t_0$ , the instant at which the peak of the pump pulses occurs.

The opto-thermal model, and all the parameters used in the simulations, are reported in Supplement 1. In Fig. 2, we report the time evolution of the probe transmission spectrum for two values of the peak intensity of the pumps. At  $I_0 = 100 \text{ MW/cm}^2$ , the PTM film barely reaches the switching temperature, therefore the probe is only slightly modulated by the pump [see Figs. 2(a) and 2(b)]. The entire thermal perturbation is approximately 1-ns long. The broadband resonant peak centered at approximately  $2 \mu\text{m}$ , which remains virtually unaltered during the pump excitation, is due to the Fabry–Pérot longitudinal resonance localized in the Si film. When the pump peak is increased to  $I_0 = 400 \text{ MW/cm}^2$ , the temperature reached in the PTM layer is higher than the transition temperature and the grating is fully formed. This implies that the GMR is still clearly visible in the probe spectrum within the broad bandwidth of the Fabry–Pérot resonance, as illustrated in Figs. 2(c) and 2(d) – see the Fano-like feature near  $\lambda_{\text{GMR}} \approx 1.93 \mu\text{m}$ . In this case, since the grating effect is strong, the Fabry–Pérot resonance is significantly modulated. We stress that the pure photoinduced phase transition [28] occurs within shorter time scales (10–100 fs) and with much larger pump peak intensities ( $\sim 100 \text{ GW/cm}^2$ ); therefore, it plays a negligible role in the photo-thermal dynamics presented here.

The guided mode acquires significant absorption losses when the PTM film is partially switched into the metallic state, leading to a relatively broad Fano resonance in the probe spectrum with a  $Q$ -factor of approximately 18. Nevertheless, the GMR abruptly appears once the pump reaches its peak ( $t = t_0 = 100 \text{ ps}$ ). The GMR is clearly visible during the relaxation time of a few nanoseconds in which the heat diffuses from the hot spots (i.e., the bright regions of the pumps interference pattern) toward the rest of the structure. Finally, the GMR gets completely quenched once the temperature in the structure has cooled below the transition temperature of  $\text{VO}_2$

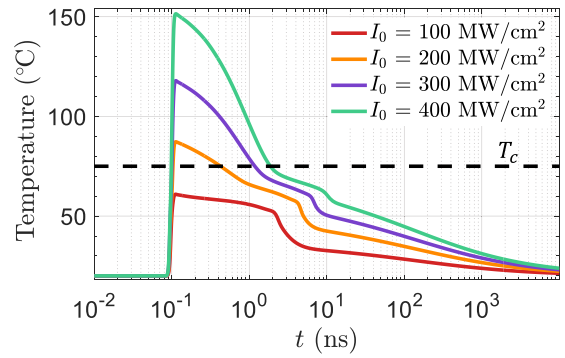


**Fig. 3.** Time evolution of the average temperature inside the  $\text{VO}_2$  film for  $I_0$  varying from 100 to  $400 \text{ MW/cm}^2$ . The average is performed across the film thickness at the position of maximum interference between the pumps. The dashed line represents the critical temperature of the  $\text{VO}_2$  film,  $T_c = 75^\circ\text{C}$ . At equilibrium, the metasurface is at  $T_{\text{amb}} = 20^\circ\text{C}$ .

(after approximately 6 ns). The duration of the entire thermal process, which determines the lifetime of the induced grating, is related to the choice of materials, the thicknesses of the films in the multilayer, and the pump peak intensity. Dynamic control of a Fano absorption resonance, similar to the result shown in Fig. 2(c), has been observed in helium at extreme ultraviolet wavelengths [29] using a high-intensity pulse ( $\sim 10^{13} \text{ W/cm}^2$ ) to ionize the excited state of helium and terminate the Fano resonance. In contrast, the transient resonance in our concept can appear at any desired wavelength by properly changing the interference pattern of the pump beams. The dynamics of the thermal process triggered by the pumps is illustrated in Fig. 3, where the time evolution of the average temperature inside the  $\text{VO}_2$  film is plotted for different values of the pump peak intensity. This analysis shows that there is a threshold value of pump peak intensity to trigger the GMR metasurface, which, for this structure, is in the range between 100 and  $200 \text{ MW/cm}^2$ . The duration of the metasurface effect, and therefore its deactivation time, grows with the pump peak intensity, being approximately 1 ns for  $I_0 = 200 \text{ MW/cm}^2$ , 3 ns for  $I_0 = 300 \text{ MW/cm}^2$ , and 6 ns for  $I_0 = 400 \text{ MW/cm}^2$ . The primary mechanism for heat dissipation is thermal conduction through the substrate, as discussed in Supplement 1, where the peculiar trend of the temperature decay during relaxation is also explained.

The spatial distributions of temperature and refractive index after the pump pulse has stimulated the PTM film and induced the metasurface are reported in Fig. 4. The induced index modulation is shallow for a pump intensity of  $I_0 = 100 \text{ MW/cm}^2$  [see Fig. 4(b)] and deeper for  $I_0 = 400 \text{ MW/cm}^2$  [see Fig. 4(d)]. The red contour line in the  $\text{VO}_2$  layer highlights the points in which the temperature is equal to the switching temperature of the  $\text{VO}_2$  film,  $T = T_c = 75^\circ\text{C}$  [30]; therefore, this line defines the boundary between the region of the film that has switched into the metallic phase ( $T > T_c$ ) and that in the insulating phase ( $T < T_c$ ). As one can observe in Fig. 4(b) and Fig. 4(d), the photo-thermally induced grating may acquire an intricate shape and size, with intermediate states of the PTM across the line at  $T = T_c$ . For  $I_0 = 100 \text{ MW/cm}^2$ , the thermally induced index modulation is shallow, and the grating effect is barely induced [see Figs. 4(a) and 4(b)]. Therefore, light can only weakly couple to the GMR. However, a more intense pump of  $I_0 = 400 \text{ MW/cm}^2$  induces a



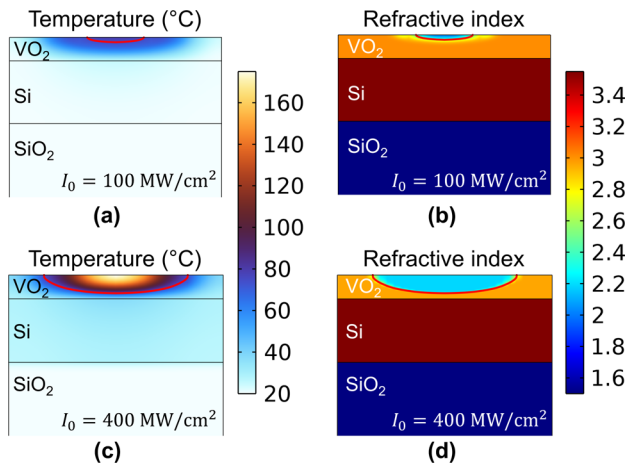


**Fig. 4.** (a) Spatial distribution of temperature after the pump has heated the PTM film ( $I_0 = 100 \text{ MW/cm}^2$ ) and induced the grating, at  $t = 0.2 \text{ ns}$ . The red line is the contour level where  $T = T_c = 75^\circ\text{C}$ . (b) Induced profile of the refractive index at the same instant for a probe wavelength  $\lambda_{\text{GMR}}$ . The light blue region in the top layer is the portion of PTM film that has switched into the metallic phase. (c) and (d) same as panels (a) and (b), respectively, for  $I_0 = 400 \text{ MW/cm}^2$  at  $t = 0.5 \text{ ns}$ .

deeper grating effect and a stronger coupling to the GMR [see Figs. 4(c) and 4(d)].

**Conclusions.** We have unveiled the dynamics of transient metasurface effects in planar multilayers hosting a PTM film of  $\text{VO}_2$  by using a pump–probe illumination scheme. We have demonstrated that a transient Fano resonance associated with the dynamic excitation of a GMR can be induced at relatively modest pump peak intensities. The coupled opto-thermal model shows activation times of the order of 10 ps for the induced metasurface effects, and deactivation times of the order of a few nanoseconds. Although here we have shown the concept of transient grating metasurface in a configuration with one-dimensional modulation of the refractive index, similar effects can be induced in two-dimensional configurations by using different light pumping schemes. We foresee the use of multilayer PTM films as a new platform to induce time-varying response in photonic resonators, dynamic control of the  $Q$ -factor, and for the development of efficient and compact light modulators and switches.

**Funding.** North Atlantic Treaty Organization (SPS G5850); Australian Research Council, Centres of Excellence Program, ARC Centre of Excellence for Transformative Meta-Optical Systems (TMOS) (CE200100010).

**Disclosures.** The authors declare no conflicts of interest.

**Data availability.** Data are available upon request to the authors.

**Supplemental document.** See Supplement 1 for supporting content.

## REFERENCES

1. A. Overvig and A. Alù, *Laser Photonics Rev.* **16**, 2100633 (2022).
2. A. Hessel and A. A. Oliner, *Appl. Opt.* **4**, 1275 (1965).
3. P. Vincent and M. Nevière, *Appl. Phys.* **20**, 345 (1979).
4. U. Fano, *J. Opt. Soc. Am.* **31**, 213 (1941).
5. S. S. Wang and R. Magnusson, *Appl. Opt.* **32**, 2606 (1993).
6. L. Mashev and E. Popov, *Opt. Commun.* **55**, 377 (1985).
7. G. A. Golubenko, A. S. Svakhin, V. A. Sychugov, and A. V. Tishchenko, *Sov. J. Quantum Electron.* **15**, 886 (1985).
8. D. Rosenblatt, A. Sharon, and A. A. Friesem, *IEEE J. Quantum Electron.* **33**, 2038 (1997).
9. Y. Ding and R. Magnusson, *Opt. Express* **12**, 5661 (2004).
10. R. Magnusson, Y. Ding, K. Lee, D. Shin, P. S. Priambodo, P. P. Young, and T. A. Maldonado, in *Nano- and Micro-Optics for Information Systems*, Vol. 5225 (SPIE, 2003), pp. 20–34.
11. J. Salcedo, A. Siegman, D. Dlott, and M. Fayer, *Phys. Rev. Lett.* **41**, 131 (1978).
12. G. D. Goodno, G. Dadusc, and R. D. Miller, *J. Opt. Soc. Am. B* **15**, 1791 (1998).
13. T. F. Crimmins, A. Maznev, and K. A. Nelson, *Appl. Phys. Lett.* **74**, 1344 (1999).
14. F. Hofmann, M. P. Short, and C. A. Dennett, *MRS Bull.* **44**, 392 (2019).
15. E. Sistrunk, J. Grilj, J. Jeong, M. G. Samant, A. X. Gray, H. A. Dürr, S. S. Parkin, and M. Gühr, *Opt. Express* **23**, 4340 (2015).
16. A. Tripathi, J. John, S. Kruk, Z. Zhang, H. S. Nguyen, L. Berguiga, P. R. Romeo, R. Orobtschouk, S. Ramanathan, Y. Kivshar, and S. Cuffe, *ACS Photonics* **8**, 1206 (2021).
17. Z. Yang and S. Ramanathan, *IEEE Photonics J.* **7**, 1 (2015).
18. M. A. Kats, D. Sharma, J. Lin, P. Genevet, R. Blanchard, Z. Yang, M. M. Qazilbash, D. N. Basov, S. Ramanathan, and F. Capasso, *Appl. Phys. Lett.* **101**, 221101 (2012).
19. M. A. Kats, R. Blanchard, P. Genevet, Z. Yang, M. M. Qazilbash, D. N. Basov, S. Ramanathan, and F. Capasso, *Opt. Lett.* **38**, 368 (2013).
20. A. Tognazzi, M. Gandolfi, B. Li, G. Ambrosio, P. Franceschini, R. Camacho-Morales, A. C. Cino, C. Baratto, D. de Ceglia, D. Neshev, and C. D. Angelis, *Opt. Mater. Express* **13**, 41 (2023).
21. B. Li, R. Camacho-Morales, N. Li, A. Tognazzi, M. Gandolfi, D. de Ceglia, C. D. Angelis, A. A. Sukhorukov, and D. N. Neshev, *Photonics Res.* **11**, B40 (2023).
22. D. Ruzmetov, K. T. Zawilski, V. Narayanamurti, and S. Ramanathan, *J. Appl. Phys.* **102**, 113715 (2007).
23. F. J. Morin, *Phys. Rev. Lett.* **3**, 34 (1959).
24. M. M. Qazilbash, A. A. Schafgans, K. S. Burch, S. J. Yun, B. G. Chae, B. J. Kim, H. T. Kim, and D. N. Basov, *Phys. Rev. B* **77**, 115121 (2008).
25. C. Giannetti, M. Capone, D. Fausti, M. Fabrizio, F. Parmigiani, and D. Mihailovic, *Adv. Phys.* **65**, 58 (2016).
26. D. Marcuse, *Theory of Dielectric Optical Waveguides* (Academic Press, 1974).
27. D. Rocco, M. Gandolfi, A. Tognazzi, O. Pashina, G. Zograf, K. Frizyuk, C. Gigli, G. Leo, S. Makarov, M. Petrov, and C. De Angelis, *Opt. Express* **29**, 37128 (2021).
28. A. Cavalleri, C. Tóth, C. W. Siders, J. A. Squier, F. Ráksi, P. Forget, and J. C. Kieffer, *Phys. Rev. Lett.* **87**, 237401 (2001).
29. A. Kaldun, A. Blättermann, V. Stooß, S. Donsa, H. Wei, R. Pazourek, S. Nagele, C. Ott, C. D. Lin, J. Burgdörfer, and T. Pfeifer, *Science* **354**, 738 (2016).
30. C. Wan, E. H. Horak, J. King, J. Salman, Z. Zhang, Y. Zhou, P. Roney, B. Gundlach, S. Ramanathan, R. H. Goldsmith, and M. A. Kats, *ACS Photonics* **5**, 2688 (2018).